Electrical Power and Energy Systems 157 (2024) 109875

Contents lists available at ScienceDirect

International Journal of Electrical Power and Energy Systems

journal homepage: www.elsevier.com/locate/ijepes

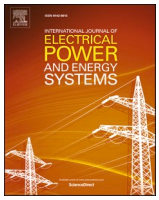

Assessment of the synthetic inertial response of an actual solar PV power plant

Raquel Villena-Ruiz [a,*], Andrés Honrubia-Escribano [a], Jesús C. Hernández [b], Emilio Gómez-Lázaro [a]

[a] Renewable Energy Research Institute and DIEEAC-ETSII-AB, Universidad de Castilla-La Mancha, 02071 Albacete, Spain
[b] Department of Electrical Engineering, Universidad de Jaén, 23071 Jaén, Spain

ARTICLE INFO

Keywords:
Grid code
Inverter
Renewable energy
Solar PV
Synthetic inertia

ABSTRACT

As the large-scale integration of renewable energy grows, inertia in power systems is reduced, which causes the rate of change of frequency to increase and worsens the frequency nadir during disturbances. There is, therefore, an urgent need to accelerate the development of international standards and regulations that require solar PV systems and other renewable installations to also contribute to stability in the network by emulating inertia. Spain is a pioneer in this field: it is currently the only country that includes the synthetic inertia technical requirement in its grid code. In this context, the present paper analyzes the synthetic inertial response of a PV system model that forms part of an actual PV power plant in Spain under two scenarios, according to its grid code: i) when measurements are conducted at the power conversion PV system level and hence only its control algorithms are executed; and ii) when measurements are conducted at the power plant level and the power plant controller also influences the response of the entire installation. Among its aims, this paper seeks to thoroughly assess the response of an actual PV power conversion system that has the capability of actively contributing to frequency regulation in a network and to critically analyze the suitability of having a power plant controller when the PV facility contributes to power-frequency control by means of an inertial response. The results reveal, at the power conversion PV system level, that the inertia emulation module significantly reduces the response times of the installation to changes in frequency -by more than 68% in the worst case under frequency increases, and by 73% under frequency decreases, thus contributing to more rapid power-frequency regulation in the network. However, at the power plant level, the power plant controller disturbs the PV power conversion system's behavior and causes the opposite effect: response times increase -up to more than 7% in the most unfavorable case when the inertia module is enabled.

1. Introduction

The introduction section is organized as follows. Section 1.1 describes the current situation regarding the presence of Variable Renewable Energy (VRE) in power systems. It also addresses the main challenges -with a particular emphasis on the loss of inertia that countries are facing to correctly integrate these renewable resources to maintain the reliability of power systems, focusing on the case of Spain. Section 1.2 details the main scientific contributions on the emulation of inertia in Photovoltaic (PV) systems, and finally, Section 1.3 summarizes the contribution and novelty of the paper and defines its structure.

1.1. Motivation and incitement. Development of the new Spanish grid code

According to the International Energy Agency (IEA), the integration of VRE into countries' power systems can be divided into different phases, characterized by penetration level and by technical, regulatory, market and institutional integration challenges. These phases range from phase 1, in which the share of VRE in the system is insignificant, with effects being at a very local level, to phase 6, in which large energy storage systems will be required to cope with the very high share of VRE [1]. In phase 4, the share of VRE is already high and significant operational and regulatory modifications are required. In countries at phase 4,

* Corresponding author.
E-mail addresses: raquel.villena@uclm.es (R. Villena-Ruiz), andres.honrubia@uclm.es (A. Honrubia-Escribano), jcasa@ujaen.es (J.C. Hernández), emilio.gomez@uclm.es (E. Gómez-Lázaro).

https://doi.org/10.1016/j.ijepes.2024.109875
Received 12 July 2023; Received in revised form 19 December 2023; Accepted 12 February 2024
Available online 21 February 2024

it is urgent to adapt the regulatory documents for VRE-based technologies to provide system services and respond appropriately to changes in generation and demand. Although most countries are still at phase 1 or 2, in others, such as Denmark or Spain, the penetration level of VRE is already very high, and hence immediate substantial modifications in the regulatory frames that govern the operation of renewable power plants are required.

At technical and operational level, the requirements demanded for grid connection of generators are typically established in documents known as grid codes. The measures to enable the achievement of greater power system flexibility as the share of VRE increases will, therefore, have to be reflected, first and foremost, in these normative documents. In the European Union (EU), a set of three grid codes, known as Network Connection Codes (NCC), were released in 2016:i) Regulation EU 2016/631 [2], establishing a network code on requirements for grid connection of generators; ii) Regulation EU 2016/1388 [3], establishing a network code on demand connection; and iii) Regulation EU 2016/1447 [4], establishing a network code on requirements for grid connection of high voltage direct current systems and direct current-connected power park modules. Drawing on these NCCs, the member countries have developed their own grid codes. In Spain, Royal Decree (RD) 647/2020 of July 7 [5] and Ministerial Order (MO) TED/749/2020 of July 16 [6] are the official documents resulting from the national adaptation of the NCCs. This grid code includes the requirements for grid connection of synchronous power-generating modules, power park modules and offshore power park modules; i.e., all types of electricity generation facilities.

RD 647/2020 [5] regulates certain aspects required for the implementation of the grid codes, while MO TED/749/2020 [6] defines the technical requirements with which generation facilities must comply. However, these documents do not contain information on the compliance process evaluation, nor on the certification methods of the power plants. Therefore, an additional document was released to coordinate the process of compliance monitoring of the NCCs, in particular, to monitor compliance with the technical requirements defined in MO TED/749/2020 [6]. This document is the Spanish technical supervision standard, 'Norma Técnica de Supervisión' (NTS) [7], the latest edition of which was published in July 2021.

MO TED/749/2020 and the NTS contain information on how the electricity generation facilities that are to be connected to the network must behave under different types of disturbances. The requirements to be evaluated in the installations include power regulation under both over-frequency and sub-frequency periods, reactive power control through different methods, Fault-Ride Through (FRT) capability and reactive power capability. Moreover, there is a specific requirement for power-generating modules that do not have an inherent capability to resist or slow down frequency deviations, i.e., for those non-synchronous modules lacking 'natural' inertia. This requirement is the capability of providing synthetic inertia.

Synthetic inertia, also known as virtual inertia or hidden inertia, is the artificial inertial behavior emulated by renewable generation units that are decoupled from the grid by electronic converters [8]. More technically, inertia emulation consists of the electronic converters responding with increases or decreases in active power proportional to the time derivative of grid frequency [9].

The Spanish grid code includes not only the synthetic inertia requisite but also the methodology to be followed by PV power plants in Spain in order to comply with it. Nonetheless, rather than being a mandatory requirement, it is currently of voluntary application. In this sense, it can be stated that Spain is a pioneer in the inclusion of the synthetic inertia technical requirement in its grid code, since the EU, in Regulation EU 2016/631 [2], refers to the requirement but the choice and discretion on how to apply it and under what conditions is left to each country. In other countries, such as Germany, Italy or the UK, where the penetration of renewable energy is also very high, discussions have started to take place about the synthetic inertia requirement. However, it has not yet been included as a requisite in their grid codes, not even as an 'optional requirement'.

Until now, frequency control in a power system was typically conducted by synchronous generators, which, in addition, provided inertia to the system because of their rotor masses. Nevertheless, as the integration of VRE grows, power systems' inertia is reduced, and the rate of change of frequency increases when the system is subjected to disturbances such as increase or loss in the generation or demand. This makes it more difficult to control synchronism of the power system and results in having a less robust system to cope with those sudden large imbalances between generation and demand. This is, therefore, one of the main reasons why additional frequency control is required and VRE based technologies should also contribute to this issue and provide inertia to the system.

In this new scenario, in which the share of VRE in power systems is already reaching significant proportions, and with a future that is shaping up to be even more ambitious in terms of the presence of clean generation sources, it is necessary for these technologies to also contribute to the regulation of power frequency. In Spain, wind and solar PV power are the renewable technologies with the greatest presence in the electricity system. In the particular case of PV power, its global market grew significantly in 2022. The total cumulative installed PV power capacity increased from 942 GW at the end of 2021 [10] to 1185 GW at the end of 2022 [11]. In this context, China is the global leader, with 414.5 GW installed, accounting for more than one third of the world PV power capacity. In the EU, which continued to grow strongly, Spain was the largest market for PV power in 2022, with an estimated 8.1 GW annual installed capacity, and is ranked first worldwide in PV penetration, contributing to the electricity demand with a penetration level of 19.1% in 2022 [11].

In this context, the present paper analyzes the synthetic Inertial Response (IR) of a specific PV power conversion system model that forms part of an actual PV power plant in Spain. It does so in two different scenarios: i) analyzing its response when only the control algorithms of the PV power conversion system itself are considered; and ii) analyzing the IR response of the complete PV power plant when also considering the control actions of the Power Plant Controller (PPC). The simulations required to assess the compliance of the facility with this 'inertia emulation' requirement are conducted, and the methodology that must be followed is described, as well as the main control algorithms that govern the operation of the PV system when providing the inertial response. In this work, the synthetic inertia support is provided by a PV system with no Energy Storage System (ESS) -or battery bank. This means that, in the face of a frequency decrease, if the generating unit is to be able to increase the active power injection, it will be necessary to "cap" its operation, or, in other words, to have it operating in a de-loaded control mode. Otherwise, if the system is already operating at its rated power -or at a setpoint near the available power, this increase in power will not be possible -or it will be possible only up to the maximum available power. In order to increase the theoretical basis of the paper, however, this study also shows a typical configuration of solar PV system equipped with an ESS, as will be seen later in the document.

The PV installation analyzed has, therefore, the capability to contribute to power-frequency regulation in a network with an IR. However, as things stand, it is up to the Transmission System Operator (TSO) to give the final go-ahead for the PV facility to make a real contribution to the power-frequency inertial regulation in the Spanish market. In this sense, a major concern arises: currently, as the contribution to power-frequency regulation of PV power plants is not remunerated, what are the incentives for owners to have power conversion PV systems equipped with this technology? Indeed, in Spain, unlike in other European countries, such as France, Belgium, Netherlands, Germany, the United Kingdom or Denmark, and as detailed in [12], the actions carried out by the power plants to contribute to primary frequency control are not remunerated, although it is mandatory for them to have that capability.

Therefore, the answer to the question raised is not simple. Although not mandatory for the time being, there is no doubt that the inertia emulation requirement will be included in the new Spanish grid code in the near future. This is prompting PV power converters manufacturers to step up their efforts and be prepared to respond appropriately when this requirement becomes mandatory.

1.2. Literature review

The scientific literature includes several contributions related to the synthetic-or virtual inertia requirement in PV installations or in other renewable energy power plants. For example, in [13], the authors conduct a literature review of the most up-to-date virtual inertia implementation techniques in Renewable Energy Source (RES) units. Primarily, the paper analyzes these techniques descriptively and at the control algorithm level. In [14], the authors also conduct a review, although, in this case, they do so by focusing on the inertia values of electricity systems in different countries, including also the damping factor evolution and a description of the most common frequency control strategies implemented in RES-based power plants, mainly in wind power plants. The work in [15] conducts, like the previous studies, a review of the strategies followed by power conversion PV systems to emulate inertia, presenting a clear summary of the main virtual inertia techniques implemented in these power electronic converters and their functioning.

A number of papers have also been published on the scheduling of the operation of power systems with a high presence of renewable energy generation plants, which must be able to provide the system, as effectively as conventional power plants, with synthetic inertia, as well as ensure an adequate response during power-frequency control. In [16], the uncertainty in power generation by wind and solar PV installations is estimated using a deep learning approach. Furthermore, in the article, this uncertainty is taken into account when scheduling grid operation, and all this with the overall objective that these RES-based power plants are also able to provide inertia to the system, as well as frequency response support. The results of the article show how the operation of the test system analyzed, in terms of safety related to frequency control, is improved, and how, in this way, costs are reduced. Other interesting articles that address the topic of synthetic inertia in renewable installations include [17,18]. Both propose models to estimate the synthetic inertia and power-frequency control responses to be provided by the generating units analyzed, although in the case of [17] the authors focus on wind power. Thus, in [17], the inertia and power-frequency requirements of an IEEE test system under different wind penetration levels are estimated in a daily framework -wind generation uncertainty is also characterized, as well as the synthetic inertia and power frequency responses that, under these scenarios, the wind power plants that form part of the test system have to provide. In [18], taking a microgrid as a basis for the study, the authors propose a model, which has the capability of providing synthetic inertia, that optimizes the operation of different distributed energy resources to meet the power-frequency regulation requirements in the grid. The results show how the rate of change of frequency and the frequency nadir during frequency disturbances improve.

The rest of the scientific articles related to the study of synthetic inertia in PV systems deal, for the most part, with the design of control strategies aimed at providing this type of IR, although they do so from different perspectives.

The control dynamics of the Direct Current (DC)/DC converter and the DC/Alternating Current (AC) inverter that form part of a PV system, as well as the dynamics of the virtual inertial controller implemented, are analyzed in detail in [19]. The whole system is simulated using the MATLAB/Simscape Power System toolbox. The design parameters are modified to study their impact on the stability of the system. The main parameters established in different grid codes to assess frequency stability are considered in [20] to analyze the performance of a combined strategy for the virtual inertia and frequency damping control in PV systems. The validation of the control strategy is then validated by means of dynamic simulations.

Other articles, also based on the design of control strategies in PV systems focus more, however, on the management of the power available in ESSs coupled to these renewable systems to provide an IR for network frequency support. For example, a synthetic inertia control in PV systems is proposed in [21] to deliver the required power through the use of a hybrid ESS, with the results being validated through simulations. The authors in [22] present a control strategy, based on the use of a supercapacitor as an ESS, to emulate inertia, and with the aim of also providing a primary frequency response. Meanwhile, in [23], the researchers propose a control strategy of supercapacitors to improve the stability of PV-based systems in standalone operation, analyzing the operation of the strategy theoretically through the use of the multidisciplinary and educational software tool MATLAB/Simulink. Lastly, the work in [24] also aims to design a control method to provide virtual inertia, although, in this case, the strategy is based on the use of the power available in the DC-link of the PV inverter.

Other works, such as [25,26], analyze the operation of PV systems, focusing on the management of power reserves. The main goal of [25] differs from the aim of the present study, since PV systems are used, in that case, to design a frequency control strategy aimed at reserving power for grid frequency support, all of this through the prediction of the system frequency using a machine learning model. The results primarily focus on analyzing the frequency response of the system under different scenarios, and not on the active power response of the system itself. The work in [26] is in the same line as the previous one, since it focuses on the design of a power reserve control in PV systems for grid frequency support, modeling, as well, a specific strategy to allow the system to operate in different modes.

The authors of the present work also have extensive experience in analyzing the response of solar PV systems to different types of disturbances, as well as studying how these types of systems provide primary frequency control and dynamic grid support. In [27], they implemented a positive-sequence model representing a utility-scale PV system -based on the generic model developed by the Western Electricity Coordinating Council (WECC), which is integrated into the IEEE 39-bus system. Both the PV system and the network are then simulated when subject to different contingencies under a variety of scenarios. In [28], the authors of the present contribution also implemented a utility-scale PV system, together with a hybrid ESS, to provide primary frequency control, including this time, however, both a statism response and an IR. The PV system modeled, also based on the generic model developed by the WECC, albeit including a number of new functionalities, is analyzed by means of transient stability analyses when coupled to the IEEE 39-bus transmission system.

The work conducted by the authors of the present paper in [29,30] is focused on the evaluation of actual PV power plants in compliance with the technical requirements established in a national grid code; in particular, in the Spanish grid code. On the one hand, the compliance of a real solar PV power plant with a number of technical requirements -such as power-frequency, reactive power control and reactive power capability requirements included in the Spanish grid code is analyzed in [29]. The paper also delves deeper into the process of compliance of the renewable facility with the Spanish grid code. On the other hand, in [30], the authors propose the use of an aggregated PV power plant simulation model as a new tool to be used during the process of evaluating the compliance of new solar PV installations with the requirements established in the Spanish grid code. The aggregated model proposed is almost ten times faster than the one described, and allows the certification and commissioning processes of new solar PV power plants in Spain to be sped up.

Nevertheless, there are noteworthy differences between the previous studies conducted by the authors and the present contribution. In the first two articles [27,28], a generic PV system, instead of a real one, is

simulated, and, additionally, only in [28] is the synthetic IR of the system analyzed. Moreover, the PV system is not simulated, in either of the two articles, according to any requirement included in any national grid code. In the second two articles cited above, [29,30], although the dynamic simulations are conducted according to the provisions of the Spanish grid code, the emulation of inertia is not a feature of the PV system under study.

The present paper serves to continue the work already conducted by the authors in [27–30]. Thus, it widens the scope of [27,28] because the contribution seeks to analyze the response of a PV system from, on this occasion, a realistic perspective, and details how the inertia emulation requirement is considered in current national regulations. Finally, it can be stated that the present work also complements the work carried out by the researchers in [29,30], since it goes beyond the mere analysis of mandatory requirements and analyzes one of the most advanced requirements that could be demanded of PV power plants, which is not actually mandatory yet in any network code worldwide.

1.3. Contribution and organization of the study

In light of the information discussed in the previous sections, there is clearly an urgent need to accelerate the development of international standards and regulations that require PV systems and other renewables to contribute to power frequency regulation in the network by emulating inertia. Additionally, it is also clear that the scientific articles published on the topic of synthetic inertia in PV installations mainly focus on the review of control strategies or the proposal of specific control methods –validated, in many cases employing a simulation tool. Hence, these papers have a high theoretical component, and the control approaches designed are not usually developed on the basis of any grid code, nor are the responses of the PV systems evaluated according to these national normative documents. Moreover, most of the papers published focus on analyzing how the frequency of the simulated network is affected by the IR provided, and not on the power response of the control device itself. Additionally, because of the very high practical applicability of the topics addressed in the study, this is a contribution of special interest to industry. Under this framework, the aims of the present paper are as follows: i) to provide the scientific world with a work that provides a real perspective on inertia emulation by renewable installations, that serves to complement existing studies in this field and that demonstrates that this is a critical requirement which, in the very near future, will be included in the grid codes of many countries; ii) to mitigate the lack of information about real experiences in the compliance evaluation process of PV systems with the synthetic inertia requirement established in a national grid code; iii) to present the methodology followed and the specific set of analyses required for an actual PV power plant to comply with this requirement and have the capability of actively contributing to frequency regulation in a power system by emulating inertia -based on the Spanish grid code; iv) to evaluate the current status of the synthetic inertia capability requirement included in grid codes worldwide, as well as the existence of mandatory or non-mandatory compliance; v) to highlight the challenges currently faced by renewable facilities' owners and to identify future trends regarding compliance with the virtual inertia requirement included in grid codes; vi) to analyze the simulation responses of an actual PV system equipped with the necessary control strategy to provide an IR; vii) analyzing the response of the PV power plant as a whole when taking into account, in addition to the power conversion PV systems designed with the capacity to provide an IR, the PPC of the installation; and viii) to critically analyze the suitability of having a PPC when the power plant contributes to the power-frequency control by means of an IR.

The paper is structured as follows: Section 2 describes how load variations affect frequency in a power system, introduces the concept of inertia and summarizes how frequency control is currently being carried out in power systems by both conventional and renewable energy power plants. Section 3 presents the methods followed to conduct the analyses performed in this contribution, presenting, as well, the configuration of the PV system under study and its control algorithms. Section 4 describes the results obtained when submitting the PV system to the synthetic inertia requirement included in the Spanish grid code. Finally, Section 5 summarizes the main conclusions obtained.

2. Power-frequency control and inertia in PV power plants

In a system comprising a shaft connecting a turbine and a generator, with a constant mechanical torque applied, two situations could occur: i) if the load (or demand) were to increase, the electrical torque would increase, the system would begin to slow down and the electrical frequency would decrease; and ii) if the load were to decrease, the electrical torque would decrease, the system would begin to accelerate and the electrical frequency would progressively increase [31]. Under this framework, given that there are a large number of generators that contribute to electricity generation in a network, frequency control must be addressed globally throughout the power system. There is, thus, a need for a control system to regulate the mechanical power applied to the turbines connected to the synchronous generators in order to maintain the electrical frequency of the system stable, at all times, in response to any variation in demand. Hence, two main variables are intended to be controlled through the power production of the generators that are part of a power system: frequency and power flow through lines. In addition to balancing generation and demand, the power generated by each power plant must also be based on the functioning of the electricity market, which primarily establishes how much power each generating unit must inject and how much power should be exchanged between neighboring control areas [32].

Nevertheless, as can be deduced from a Primary Frequency Control (PFC) action [32] -also usually referred to as Frequency Containment Reserve (FCR), the power generated by a conventional generating unit is not immediately adapted to the new situation in which the load has changed. Therefore, in the event of an increase in the load, the amount of energy required instantly to compensate for this load increase comes from the kinetic energy of the rotating masses of the generators, the speed of which starts to decrease. This is the so-called *inertial response*. In this regard, the inertia constant, usually represented by the letter H, is a key parameter in electric power systems. In a generator, H is defined as the kinetic energy stored in the rotating mass at synchronous speed, divided by the rated power of the machine, as shown in Eq. (1) [33,34].

$$H = \frac{J\omega_r^2}{2S_r} \tag{1}$$

where J is the moment of inertia ($kg \cdot m^2$), ω_r is the rated mechanical angular speed (rad/s), and S_r is the rated apparent power of the generator ($V\,A$).

H can be expressed in $MWs/MV\,A$, although if a change of base is made and the inertia constant is defined as a function of the base power of the system, it can be expressed in seconds (s) or in the per unit system (p.u.), as explained in [35,36]. The inertia constant indicates, intuitively, the inertia of a generator regardless of its rated power.

Turning to the subject of the PFC, in conventional power plants, to contribute to this control action, the governors of the turbines act to control flow in the inlet valve and thus control output power. However, in most renewable energy power plants, which are electronically interfaced, there are neither turbines nor large synchronous generators. PFC is, therefore, not carried out through the regulation of an input flow rate, but through the operation of the power electronic converters that form part of the renewable generation devices. In the case of PV power plants, to contribute to power-frequency regulation, the droop control mode is followed, as in conventional power plants [34]. A droop –or statism– constant (R) must be configured in each PV power conversion system according to the applicable grid code. R is defined as the speed increase of the machine ($\Delta\omega$) divided by the power output increase (ΔP), and

with a minus sign so that it is always positive, as can be observed in Eq. (2) [34].

$$R = -\frac{\Delta\omega}{\Delta P} \tag{2}$$

R is typically expressed in percentage. For instance, a statism value of 3% means that a decrease in frequency of 3% causes a 100% increase in generated power.

In this way, the power-generating modules will be capable of activating the provision of active power frequency response when changes in this last variable occur [29], in the same way as conventional power plants do.

Thus, when frequency rises occur in the network, PV power plants must guarantee a reduction of their active power output. On the other hand, when frequency drops occur, these facilities must guarantee an increase in their active power output, thus seeking to constantly balance generation and demand. In the case of Spain, as indicated in Section 1, MO TED/749/2020 [6] defines, among other things, the characteristics of the power-frequency technical requirements that renewable power plants must comply with, while the technical supervision standard [7] details the compliance process evaluation of the requirements and includes information on the parameters settings. In this regard, conducting dynamic simulation analyses is one of the tools allowed to check whether a PV power plant in Spain complies with the power-frequency technical requirements [30]. This is done as a step prior to the commissioning of the facility.

Therefore, thus far, we have discussed the remarkable growth of VRE-based power plants over the past few years and the consequent reduction of inertia in power systems, highlighting the necessity for these renewable installations to contribute to grid stability in the same way as other power plants do. Moreover, the control mode followed by conventional generation facilities to contribute to power-frequency regulation has been explained, as well as the mechanism based on which PV power plants are intended to provide power-frequency support. In this regard, the concept of statism –or droop– has also been described, in addition to briefly discussing the importance of the IR of generators.

Nevertheless, just as there is a clear distinction between the inertial response of conventional power plants and their PFC action -concepts that have been discussed in the previous paragraphs, it is also necessary to make this distinction in the context of renewable installations. In other words, in PV generation, it is also necessary to differentiate the change in the PV power conversion system output power due to the established droop, which causes the power to increase or decrease at a constant rate in the face of a load variation, from the IR that attempts to be emulated through the synthetic inertia requirement. This is designed so that the PV power conversion systems respond with increases or decreases in active power proportional to the time derivative of grid frequency. The difference between these two concepts will be shown clearly in Section 4, while the theoretical background behind the synthetic inertia supply capability of a PV system is discussed at greater length in Section 3.2.

Summarizing, as inertia in power systems decreases due to the closure of conventional power plants, changes in demand have a higher impact, in the sense that frequency variations are reflected in the network more quickly; i.e., the 'dynamics' of the power system are faster. This forces the generation units to react more quickly to adapt to the new situation. All this highlights the importance of inertia in networks, as well as the need for new renewable generation plants to also be able to contribute inertia to the system.

3. Methodology

The present section describes the methods used to conduct the analyses in this work. In particular, Section 3.1 reviews the main characteristics of the analyses to be conducted when assessing the synthetic inertia capability requirement in PV power plants according to the Spanish grid code, and includes the specific values that are set to carry out the simulations in the two scenarios analyzed, when the IR is studied at the power conversion PV system level and when studied at the Point of Common Coupling (PCC) and the plant is equipped with a PPC. Section 3.2 describes the configuration of the PV system and the control algorithms that allow both the PFC and the IR to be provided by the power conversion PV systems. Finally, Section 3.3 details the layout of the PV power plant –formed by PV systems, transformers and lines and equipped with the aforementioned PPC, the capability of which to contribute to power frequency regulation in the network by providing a synthetic IR is studied.

3.1. Synthetic inertia capability requirement of the PV system according to the Spanish grid code

The NTS, which was released to monitor compliance with the technical requirements defined in Spanish MO TED/749/2020, also released a specific document with guidelines on drafting the inertia emulation report in those cases where applicable. Among other aspects, this document states that the report will only be delivered to the TSO by the generating units that have the capability of emulating this non-mandatory requirement. In this sense, the capability of providing synthetic inertia will become a mandatory requirement as soon as it is regulated as part of the balancing services of the power system.

The compliance of the generating units with this requirement can be evaluated through dynamic simulations, which are required to be conducted only at the Power Generation Unit (PGU) level, unless the Power Park Module (PPM) owner declares the existence of higher order hierarchical control at the PPM level that may impact inertia emulation control. Thus, in this case, as the PPC also has an integrated inertia module -as will be explained further on, simulations will also be required at the PPM level. It should be noted at this point that in order to carry out the aforementioned 'dynamic simulations', a validated PV power conversion system model was used. That is to say, a model that faithfully represents reality with minimum errors is used; a model the behavior of which has been ratified and accepted by the Spanish Transmission System Operator (TSO), *Red Eléctrica de España* (REE).

PGUs refer to the main generation unit that forms part of the power plant, while PPMs refer to the power plant as a whole [29]. The simulation analyses are required to show the improvement of the unit response with the inertia emulation control enabled compared to the same simulations without it enabled. In no case should the power-frequency control mode be deactivated. In particular, when conducting the dynamic simulations, the NTS states that two paths may be followed: i) performing the simulations based on the provisions of standard IEC 61400-21-1 [37]; and ii) performing an alternative set of simulations, proposed by the owner of the PPM and to be agreed with the TSO in advance. In our case, the first path has been followed.

Standard IEC 61400-21-1 describes the synthetic inertia requirement as the ability of the PGU to support the grid by providing additional active power in the case of frequency events. This capability must be tested at the PGU while operating during continuous operation at different load levels of active power (P). The three following conditions are set while conducting the different tests:

1. At a partial load between 0.25 and 0.50 times the nominal power (P_N) of the PGU.
2. At a load level above 0.80 times the nominal power of the PGU.
3. At a load level below the nominal power of the PGU. The nominal power must be equal, in turn, to the available active power (P_{av}), i.e., to the power that could be generated depending on the primary resource available.

From the above conditions it follows, therefore, that only in the third case the PGU is operating with a reduced active power reference or, in

other words, in a de-rated or de-loaded control mode. Standard IEC 61400-21-1 [37] also states that the previous load levels must be set to analyze the PV system response under two conditions, frequency increases and frequency decreases. It should be noted, at this point, that none of the normative documents states what the value of the frequency variation should be, but rather that it should be a sufficiently sharp variation to allow differences between having and not having the inertia emulation module enabled to be analyzed.

Therefore, during the test cases, different inertia parameters must be set, as well as the test conditions. Then, the measured values from the simulation results must be evaluated according to the criteria included in Standard IEC 61400-21-1. Standard IEC 61400-21-1 regulates aspects related to the measurement and evaluation of electrical parameters in wind energy generation systems [38]. However, this standard is followed because no specific methodology has been developed for PV systems. Moreover, to conduct the simulations, the PGU is connected to a fictitious network that emulates the characteristics of the actual network. The power system simulation software tool used is DIgSILENT PowerFactory version 2022.

More specifically, the synthetic inertia capability requirement is evaluated through the analysis of the time series of active power and frequency reference at the PGU terminals. Then, on the basis of the simulation results obtained, a number of parameters must be considered to assess the compliance of the PGU with the inertia emulation requirement. The most important ones are listed as follows, and are shown graphically in Fig. 1:

- Reaction time. Defined as the time elapsed from the time the control signal for activation of the PGU response is sent until the amplitude change reaches 10% of the step height of the measured output variable.
- Response time. Defined as the time that elapses from the beginning of the event -i.e., the change in the power response of the PGU until its value enters the predefined tolerance band of the target value.
- Settling time. Defined as the time that elapses from the beginning of the event -i.e., the change in the power response of the PGU until its value remains continuously within the predefined value of the tolerance band of the active power response.
- Predefined tolerance band. The tolerance band considered in the evaluation of the settling time is defined as 5% of the active power variation with which the PGU responds to the frequency change.

Once the parameter has been properly set in the PGU and all the tests have been conducted, the assessment of some of the parameters listed above determines the compliance of the PV system under study with the synthetic inertia technical requirement. Thus far, no specific criteria or limits have been developed or set for the acceptance of the results. Thus, as is currently established in the Spanish grid code, only two parameters need to be taken into account for the compliance evaluation of the system with the synthetic inertia technical requirement: the system will be considered to comply if the reaction and response times are lower with the inertia module activated.

In addition to the variables listed above, there are others the value of which will also be shown in the results section, once the simulations are performed. These are: i) default active power boost (ΔP), defined as the boost of active power when the frequency change occurs; ii) gradient of active power boost (dP/dt), defined as the rate of change in active power when the frequency change occurs; iii) steady-state time, defined as the time the system operates in steady state once the settling time has expired; iv) ramp-down time, defined as the time during which the active power value decreases from 90% to 10% of the target value; and v) recovery time, defined as the time from the end of the event after which the active power is continuously within the predefined tolerance band around the value of active power prior to the event. The time parameters just defined are also shown, graphically, in Fig. 1.

Based on the general description of the synthetic inertia tests included in the Spanish grid code and explained in the present section, four parameters must be specifically set to conduct the simulations. These are the change and gradient of frequency applied, and the inertia trigger and recovery values, defined as the frequency thresholds where the PV power conversion system will start boosting active power and will stop boosting active power, respectively.

In the case where the inertial response of the PV power conversion system is analyzed, frequency increases and frequency decreases are set to 1 Hz each. In addition, the gradient of frequency applied is set to 0.50 Hz/s in the tests under frequency increases, and to −0.16 Hz/s in the tests under frequency decreases. Finally, the values of frequency trigger and frequency recovery to assess the IR are set to 50.01 Hz and 49.99 Hz under the frequency increase and decrease tests, respectively. Table 1 summarizes the value of all these parameters (note that, in test cases 3 and 6, the system is operating in a de-loaded control mode, as mentioned previously).

On the other hand, in the case where the inertial response is analyzed at the power plant level -and in this case it is necessary because the plant controller also has an integrated inertia module that can influence the overall behavior of the installation, the load level conditions established

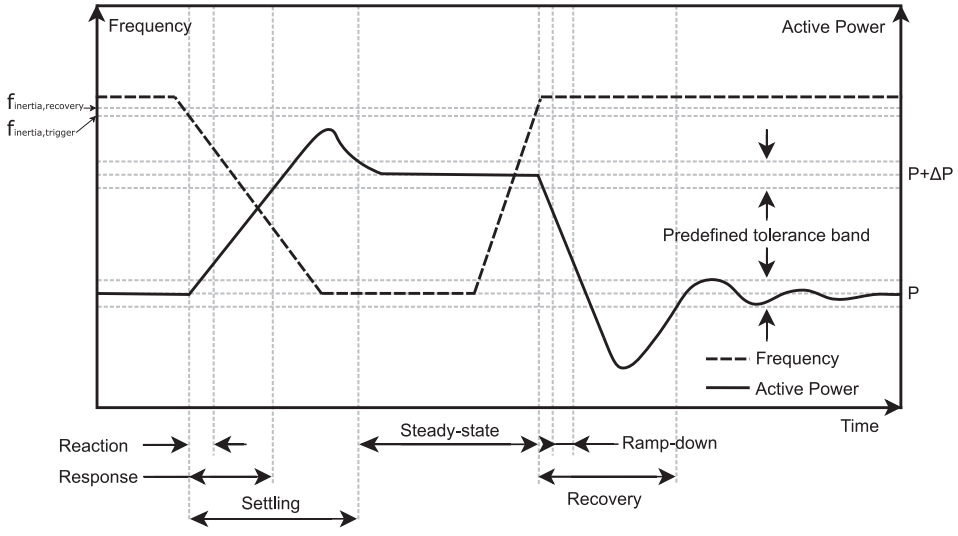

Fig. 1. Time parameters for characterization of the synthetic inertia response. Adapted from [37]

Table 1
Setting of parameters for test cases 1, 2, 3, 4, 5 & 6 to analyze the IR of the PV system.

	Frequency Increases			Frequency Decreases		
Test Case	1	2	3	4	5	6
P (pu)	0.30	0.85	0.85 ($P_{av} = P_N$)	0.30	0.85	0.85 ($P_{av} = P_N$)
Change in f Applied (Hz)	50–51	50–51	50–51	50–49	50–49	50–49
Gradient of f Applied (Hz/s)	0.50	0.50	0.50	−0.16	−0.16	−0.16
f Inertia, Trigger (Hz)	50.01	50.01	50.01	49.99	49.99	49.99
f Inertia, Recovery (Hz)	50.01	50.01	50.01	49.99	49.99	49.99

to conduct the tests have also been described in the present section. Moreover, the same types of simulations, with both the inertia module activated and deactivated, must be conducted. In this way, it will be verified whether the response time is lower or not with the inertial module enabled. In this case, the frequency increases and decreases are of 0.60 Hz each, the gradient of frequency applied is set to 0.30 Hz/s in the tests under frequency increases, and to −0.25 Hz/s in the tests under frequency decreases. The values of frequency trigger and frequency recovery to assess the IR are set to 50.01 Hz and 49.99 Hz under frequency increases and decrease tests, respectively. Table 2 summarizes the value of all these parameters (note that, as in the case of test cases 3 and 6, in test cases 9 and 12 the system is also operating in a de-loaded control mode, as mentioned previously).

3.2. Synthetic inertia supply capability: Control algorithms of the PV system

The configuration of the PV system analyzed is schematically shown in the upper part of Fig. 2 (only the area with a white background); a system which has the capability of providing synthetic inertia. It should be noted, therefore, that the system studied in the present contribution is not a hybrid system, i.e., it does not have any ESS -or battery bank. However, the real converter tested is a two-stage power conversion system (more information about this type of systems can be found in [39]), since coupling an ESS is one of the most suitable solutions that are outlined in the future for solar installations to contribute inertia to the system, and because there are real prospects of this system being coupled to the power plant in the future. Moreover, this 'typical' ESS is also shown to provide the study with a greater theoretical background.

Therefore, the system consists mainly of a PV array connected with the DC link through a PV converter, and a bidirectional Voltage Source Converter (VSC), through which the DC link is interfaced with the network. The dashed lines represent the control signals entering and leaving the control algorithms of the elements on which they act. As can be seen, and as it was explained above, in this case, the device tested is a two-stage PV power conversion system instead of a one-stage PV power conversion system [40–42]. The main reason for having this topology is so that in the future an ESS such as the one mentioned above can be coupled to it. It should be noted that this fact does not affect the final response of the system, nor does it modify the implementation or the control functions that are part of the inertial response algorithm.

The configuration has two independent control subsystems (shown in the area with white background of Fig. 2). The two control algorithms are as follows: i) the first one (the PV Converter Control Algorithm) controls the PV converter -or boost converter to track the maximum power coming from the PV array and inject it into the DC link, and is also responsible not only for contributing to PFC but also for providing an IR; and ii) the second one (the VSC Control Algorithm) controls the DC link voltage and the reactive power flow between the DC link and the network, and it does so by controlling the VSC -or PV inverter.

In particular, regarding the control algorithm implemented in the PV converter, it is worth noting that the device is not only able to contribute to PFC, but also to provide an IR. Thus, as mentioned, both the PFC and IR of the PV system are governed by the control algorithm implemented in the PV converter. This is shown graphically in Fig. 2 (please note the asterisk and the place where the acronyms IR and PFC appear).

On the one hand, in reference to the PFC capability, the algorithm implemented complies with the requirements established in the Spanish grid code, and allows the PV system to respond to changes in frequency by increasing or decreasing its output power according to the statism –or droop– established. Eq. (3) shows the active power command provided by the PFC algorithm ($\Delta P_{PFC-cmd}$) [28]. This control is shown, graphically, in the top part of Fig. 3, in dark gray.

$$\Delta P_{PFC-cmd} = -\frac{|\Delta f| - |\Delta f_{RI}|}{R \cdot f_n} \cdot P_{ref} \tag{3}$$

where Δf is the frequency deviation, Δf_{RI} is the frequency response insensitivity, P_{ref} is the actual active power output at the moment the frequency sensitive mode (FSM) is triggered -i.e., at the moment the PGU's capability to contribute to the PFC is activated, R is the statism and f_n is the nominal frequency.

Regarding the synthetic IR capability of the PV system, the algorithm is defined based on a derivative control, the performance of which is similar to those that conventional generators carry out [43]. Eq. (4) shows the active power command provided by the synthetic IR algorithm (ΔP_{IR-cmd}). This control is also shown, graphically, in the bottom part of Fig. 3, in light gray.

$$\Delta P_{IR-cmd} = -2H^* \cdot f^* \cdot \frac{df^*}{dt} \cdot \frac{P_{ref}}{f_n^2} \tag{4}$$

where H^* is the synthetic inertia constant –let us recall that the letter used to represent the inertia constant in conventional generators is H, as indicated in Section 2, with f^* being the measured value of frequency.

In Fig. 3, Δf, estimated as the difference between the reference frequency (f_{ref}) and f^*, goes through a series of control blocks through which $\Delta P_{PFC-cmd}$ is ultimately estimated, as previously indicated in Eq. (3). Moreover, within this algorithm, i.e., within the PFC capability algorithm, T_P establishes the frequency measurement accuracy, Δf_{SS-max} represents the maximum steady state frequency deviation, and LRC_{FSM} is the limit rate of the change in active power due to the FSM.

On the other hand, within the IR capability algorithm, T_D establishes the frequency derivative measurement accuracy, T_{F1} is the time constant of a low pass filter used to filter noise from the frequency data, and

Table 2
Setting of parameters for test cases 7, 8, 9, 10, 11 & 12 to analyze the IR of the PV power plant at the PCC.

	Frequency Increases			Frequency Decreases		
Test Case	7	8	9	10	11	12
P (pu)	0.35	0.80	0.90 ($P_{av} = P_N$)	0.35	0.80	0.90 ($P_{av} = P_N$)
Change in f Applied (Hz)	50–50.6	50–50.6	50–50.6	50–49.4	50–49.4	50–49.4
Gradient of f Applied (Hz/s)	0.30	0.30	0.30	−0.25	−0.25	−0.25
f Inertia, Trigger (Hz)	50.01	50.01	50.01	49.99	49.99	49.99
f Inertia, Recovery (Hz)	50.01	50.01	50.01	49.99	49.99	49.99

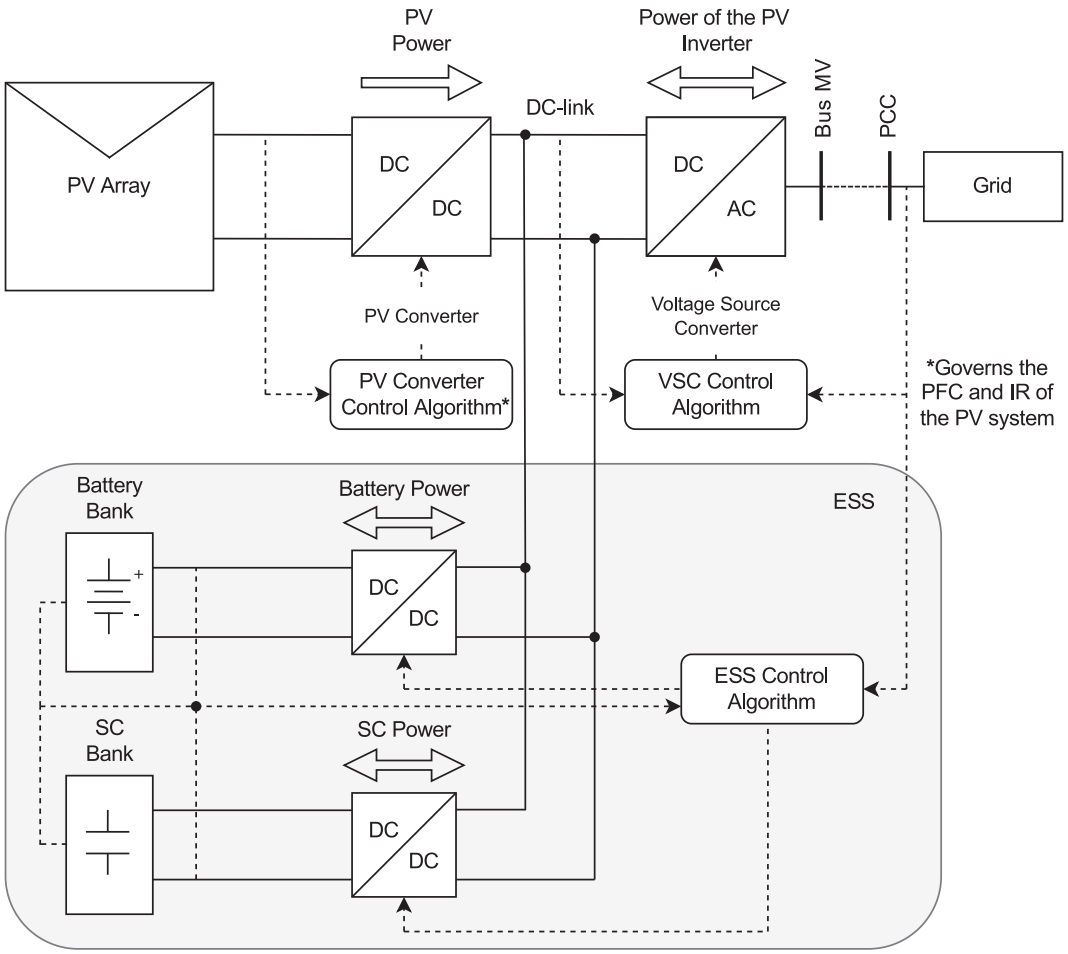

Fig. 2. Configuration of one of the PV systems analyzed (white colored area). The gray colored area represents how the system could be enhanced with an ESS.

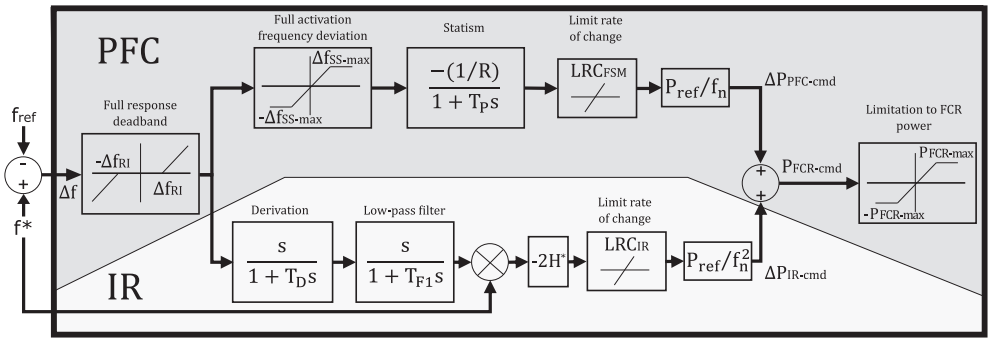

Fig. 3. Control algorithm in the PV converter. PFC and IR capability.

LRC_{IR} is the limit rate of the change in active power due to the IR control mode.

Finally, as shown in the right-hand part of Fig. 3, both the $\Delta P_{PFC-cmd}$ and the ΔP_{IR-cmd} command signals are added, and the resulting value is the FCR active power command ($P_{FCR-cmd}$), which provides both a PFC and an IR as a consequence of a change in frequency [28,43].

Most of the power conversion PV systems currently only have the capability of contributing to PFC in the power system, and therefore they only have the PFC algorithm implemented. Thus, in this case, the power conversion PV system manufacturer 'added' a new functionality, which is the capability of providing an IR, thus making the power conversion PV system behave with increases or decreases in active power proportional to the time derivative of grid frequency.

In the present contribution, the change in the output power of the PV system is determined, precisely, by the availability of active power, especially with regard to 'active power to be raised'. In other words, when a frequency rise occurs, the PV system will be required to decrease its active power injection. In this case, where the active power response is 'to be down', it is self-evident that there will be no major problem, since it is always possible to reduce the active power setpoint of an electricity generation unit. In contrast, when a decrease in frequency occurs, the PV system will be required to increase its active power injection. However, if the generation unit is already operating at its rated power, a problem may arise, since no 'extra' active power will be available to comply with the requirements demanded. This means there may be times when the PV installation will have to be 'capped' to be able

to contribute to PFC in the cases where frequency decreases. This is why it would be desirable to use ESSs in combination with PV systems equipped with PFC and IR capability: they would allow energy to be stored and would be ready to inject it into the network when frequency decreases occur.

Therefore, the trend with regard to the participation of PV power plants in the PFC of a power system is towards the use of the state-of-the-art converters in combination with ESSs, i.e., the trend is towards the deployment and operation of hybrid PV power plants. In this sense, and as mentioned above, Fig. 2 also shows, in the gray colored area, an ESS, which could be configured alongside the PV facility. The ESS is formed by a Li-ion battery bank and a supercapacitor (SC) bank. This is done to provide high energy storage and fast response time. The implementation of these hybrid systems would mitigate the effects of reduced inertia in power systems, offering power ramp rates higher than those usually required.

In this case, in which both systems would operate jointly, there would be another algorithm that would control the ESS converters, managing the available active power of the ESS at the DC link and, hence, at the PCC, thus controlling network frequency and being responsible for the PFC of the hybrid system. Overall, this approach would operate the ESS while keeping the PV system in the Maximum Power Point Tracking mode (MPPT).

3.3. PV power plant with synthetic inertia supply capability and power plant controller

In addition to analyzing the response of the PV power conversion system model that forms part of the PGU, the IR of this power electronic device is also analyzed at PPM level, i.e., considering, furthermore, the PPC of the PV power plant. The functions of the PPC are to record the network conditions, such as frequency, voltage, or active and reactive power demand, and, once these magnitudes have been recorded, its function is also to give instructions to the PV systems to act accordingly and generate the active and reactive power required. The behavior of the PPC is governed by a series of parameters set by each manufacturer, and their value is critical in establishing the resulting dynamics.

In this case, the PPC also has an integrated inertia module, although not all do. Thus, the PPC, in the event of a change in frequency, in addition to indicating to the PV systems the new power to be injected, tells them how to inject it; that is, it establishes that the power injection must vary proportionally to the time derivative of the frequency.

Therefore, measurements are taken at PPM level. The main objective of these tests is to assess the suitability of having a PPC equipped with the capability of sending control signals to the PV power conversion systems during frequency deviations in the network to contribute to PFC. The PV power plant, shown in Fig. 4, is formed by 12 PV systems of 1.637 MVA each -with IR capability, 12 Medium Voltage (MV) - Low Voltage (LV) transformers, and 1 High Voltage (HV) - MV transformer.

4. Results

The present section is divided into two subsections. In Section 4.1, the simulation responses of the PV system model are analyzed when the inertia emulation module is enabled and disabled. In Section 4.2 the behavior of the PV power plant -equipped with a PPC at the PCC level is

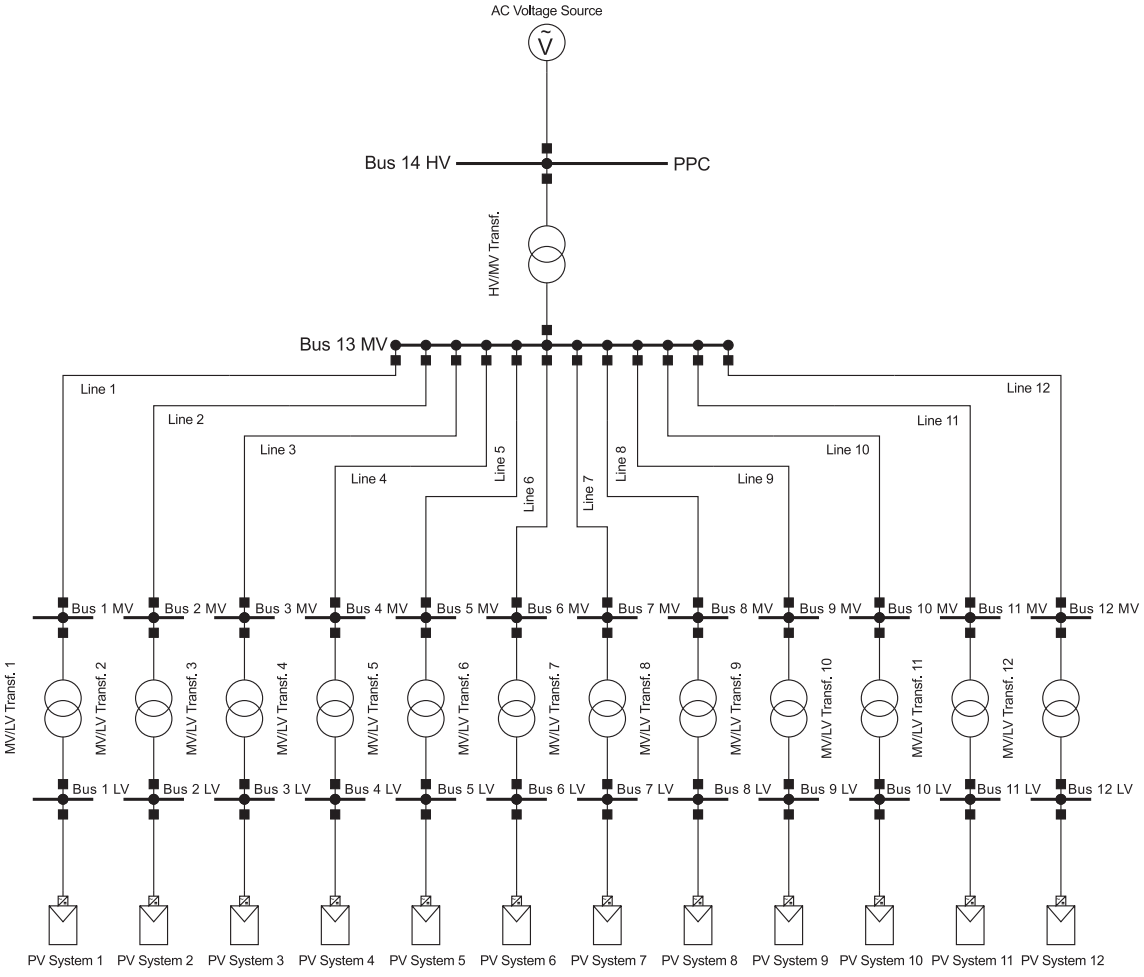

Fig. 4. Layout of the actual PV power plant tested.

then analyzed under these same two scenarios, with the inertia module activated and deactivated. In all test cases, as explained in previous sections, the PV system without ESS is studied. The definition of all the parameters evaluated in the present section is included in Section 3.1.

4.1. Evaluation of the inertial response at the PV system level

Tables 3 and 4 show the numerical results obtained once the required tests have been conducted and the measured variables have been evaluated. The definition of all these test cases and variables in included in Sections 3.1 and 3.2. In particular, Table 3 shows the results obtained when the synthetic inertia tests are conducted under frequency increases, while Table 4 shows the results obtained when those same tests are carried out under frequency decreases. In these tables, the comparison of the variables in italics, both with the inertia module enabled and disabled, determines the compliance of the evaluated system with the synthetic inertia requirement.

The simulation responses of the PV system under the test cases conducted (described in Sections 3.1 and 3.2) are shown, for frequency increases, in Fig. 5(a–c), and for frequency decreases, in Fig. 6(a–c). In all these figures, orange represents frequency, dark blue represents the active power response of the PV system when both the PFC and the IR capabilities are considered, and blue dotted lines represent the active power response of the PV system when it only contributes to PFC in the network. In addition, and by way of example, the tolerance band, defined as 5% of the active power variation with which the generating unit responds to frequency changes, is shown in Fig. 5a in light gray. In this way, the reader can have a better idea of the time parameters measured.

As can be observed in Tables 3 and 4, the reaction time measured when the inertia emulation module is activated is lower, in all cases –both under frequency increases and decreases– than the reaction time measured when the inertia emulation module is not activated. The definition of this parameter, included in Section 3.1, gives an idea of the value of the ramp slope of the PV system power response, being higher in the case where the inertia emulation module is activated, and thus contributing more rapidly to power-frequency regulation in the network. This is also evident when observing the values of the gradient of the P boost, included, as well, in Tables 3 and 4. Indeed, in both situations –when the inertia module is enabled and disabled– the default P boost value is the same, but the values of the gradient of P boost are higher when an inertial response is provided. Thus, it is clear that the predefined tolerance band is entered more quickly in this case.

On the other hand, regarding the response time, also shown in Tables 3 and 4, the values measured when the inertia module is activated are, in all cases, and as in the case of the reaction time, lower than the values measured when the module is not activated. The values obtained for the response time parameter indicate that the active power signal of the PV system enters the tolerance band of the target value earlier than in the case where inertia is not emulated.

Table 3
Numerical results of the inertia emulation test cases under frequency increases. Evaluation at power conversion PV system level.

Frequency Increases						
Test Case	1		2		3	
P Range (Test Case)	$0.25P_N < P < 0.50P_N$		$P > 0.80P_N$		$P = 85\%P_N$ $P_{av} = P_N$	
Inertia Emulation	No	Yes	No	Yes	No	Yes
Default P Boost, ΔP (pu)	−0.16	−0.16	−0.16	−0.16	−0.16	−0.16
Gradient of P Boost, dP/dt (pu/s)	−0.08	−0.25	−0.08	−0.25	−0.08	−0.26
Reaction Time (s)	0.25	0.04	0.25	0.04	0.19	0.03
Response Time (s)	1.93	0.61	2.92	0.57	1.91	0.57
Settling Time (s)	1.93	2.54	2.53	2.92	1.91	2.55
Steady-State Time (s)	3.07	2.47	2.47	2.08	3.07	2.45
Ramp-down Time (s)	0.03	0.01	0.03	0.02	0.03	0.01
Recovery Time (s)	0.00	0.00	0.00	0.00	0.00	1.00

Table 4
Numerical results of the inertia emulation test cases under frequency decreases. Evaluation at power conversion PV system level.

Frequency Decreases						
Test Case	4		5		6	
P Range (Test Case)	$0.25P_N < P < 0.50P_N$		$P > 0.80P_N$		$P = 85\%P_N$ $P_{av} = P_N$	
Inertia Emulation	No	Yes	No	Yes	No	Yes
Default P Boost, ΔP (pu)	0.00	0.00	0.00	0.00	0.15	0.15
Gradient of P Boost, dP/dt (pu/s)	0.00	0.00	0.00	0.00	0.08	0.29
Reaction Time (s)	0.00	–	0.00	0.00	0.24	0.04
Response Time (s)	0.00	–	0.00	0.00	1.78	0.47
Settling Time (s)	0.00	0.00	0.00	0.00	1.78	0.47
Steady-State Time (s)	0.00	–	0.00	0.00	3.22	4.53
Ramp-down Time (s)	0.00	0.03	0.00	0.03	0.04	0.01
Recovery Time (s)	0.00	0.15	0.00	0.65	0.00	1.03

Both the difference in the reaction time and the response time between the cases in which the inertia module is activated and deactivated can also be clearly seen, graphically, in Fig. 5a–c, corresponding to the tests in which frequency increases, and also in Fig. 6c, when frequency decreases. However, when the PV system is subject to frequency decreases in test cases 4 and 5 (Fig. 6a, 6b), the difference between the power responses with the inertia emulation module activated and deactivated are not as evident as in the other cases.

In test case 4 (Fig. 6a), the PV power conversion system does not even provide a power output change when frequency decreases from 50 Hz to 49 Hz, at least when the inertia module is deactivated (only PFC is conducted). When the inertia module is activated, there are no changes in the active power output of the PV system in the moment frequency starts to decrease, nor during the period when frequency is kept at its minimum value. The only change can be seen when frequency has already recovered its setpoint value (50 Hz), and corresponds to a rapid reduction and a subsequent recovery of the power.

In test case 5 (Fig. 6b), when the inertia module is deactivated, there is no change in active power during the frequency disturbance. However, when the inertia module is activated, something similar to what was seen in the previous case occurs. There is no change in the active power output of the PV system when frequency decreases, nor when frequency is kept at its minimum, although a sudden reduction of this power can be seen (down to a value of almost 0 pu) when frequency recovers. This reduction in active power is followed by a progressive increase up to the operating point of the PV system prior to the disturbance.

Finally, in test case 6 (Fig. 6c), in contrast to the two previous cases, there is an increase in power during the decrease in frequency when the inertia emulation module is both activated and deactivated. In this case, as frequency decreases, the output power of the PV system increases. When frequency returns back to 50 Hz, there is then a recovery period of active power when the inertia module is activated.

There is a clear explanation for the above, i.e., as to why the PV system is able to vary its power when there is an increase in frequency (Fig. 5), and why, in the first two test cases under frequency decreases (Fig. 6), it is unable to vary its power. Under frequency increases, there is no problem for the PV system to decrease the active power it is injecting into the grid (Fig. 5a–c). However, during the first two test cases under frequency decreases (Fig. 6a and b), it must be taken into account that the available power is equal to the power at which the PV system is operating. Therefore, the power conversion PV system has no more power to deliver than the power at which the tests are conducted (power can be generated depending on the primary resource available; if no more power is available, it is impossible for the PV system to generate more). In the third test case (Fig. 6c), the test is performed with the PV system operating in a de-loaded control mode (or 'capped'), i.e.,

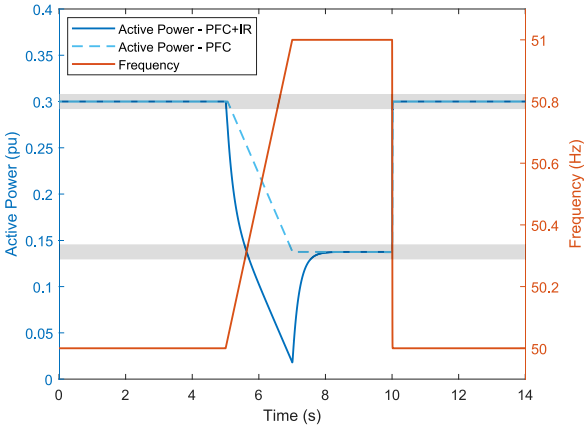

(a) Test case 1: $0.25P_N < P < 0.5P_N$

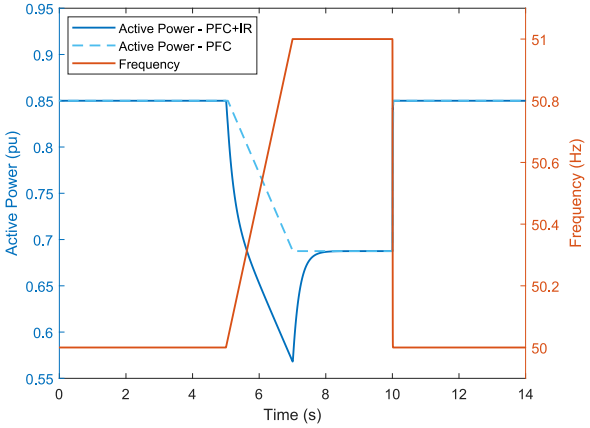

(b) Test case 2: $P > 0.80P_N$

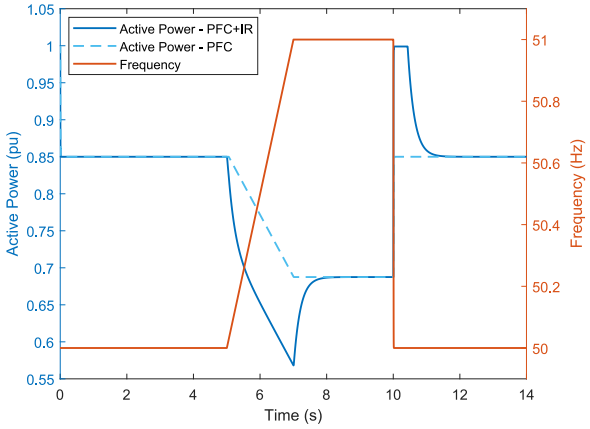

(c) Test case 3: $P = 85\%P_N; P_{av} = P_N$

Fig. 5. Synthetic inertia capability of the PV system - PFC and combined PFC & IR to frequency increases.

operating at a certain power over the available power (which is, in turn, equal to the rated power of the device, see Table 4). Thus, the PV system can increase the active power it is injecting into the grid because it is not operating at the maximum level at which it could operate.

It can also be observed that there are no recovery periods of the active power when only PFC is provided by the PV system (see the light blue dotted line in all the sub-figures of Figs. 5 and 6, in the post-disturbance period). There are also no 'overshoot' periods at the beginning of the frequency fault. This is because the PV system's behavior in this case -when only PFC is provided is governed exclusively by its statism, which makes it behave in this way. On the other hand, the only recovery period of the active power when frequency is increased during the tests and the inertia module is activated is observed for test case 3 (Fig. 5c). Under frequency decreases, something similar occurs, as the PV system only presents recovery periods of the active power when the emulation of inertia is conducted (see Fig. 6b and c). In this sense, it is important to note that, when the inertia emulation module is enabled, the PV system will respond providing an IR at the beginning and the end of the frequency fault, since the control algorithm detects both variations, the frequency reduction and its subsequent rise, and vice versa. It is for this reason that the recovery periods occur. Thus, for example, in test case 3 (Fig. 5c), when the PV system provides an IR (blue solid line), as soon as the frequency starts to rise, the power starts to decrease proportionally to the time derivative of the frequency. Subsequently, when the frequency starts to recover, falling again but more rapidly than it rose, the power also varies proportionally to the time derivative of the frequency, with the slope of the power variation being steeper in this case. With this in mind, there are no recovery periods in test cases 1 and 2 (Fig. 5a and b) for the same reason as why the PV system power does not increase in test cases 1 and 2 during the frequency fault: the available power is equal to the power at which the PV system is operating and, hence, has no more power to deliver. In contrast, in test case 3 (Fig. 5c), there is a recovery period when frequency returns to 50 Hz because the available power is higher than the power at which the PV system is operating. Finally, under frequency decreases, there are recovery periods in all test cases (Fig. 6a–c) because, when the frequency rises again, the control algorithm detects this and sends a command for the power to decrease. This is possible because the power has a margin to decrease in these cases.

Contrary to what is generally the case for the response and the reaction time values, the settling time, defined as the time that elapses from the beginning of the change in the output power of the PV system until its value remains continuously within the tolerance band defined, is higher, in almost all cases, when the inertia emulation module is activated (Table 3). As can be observed in Fig. 5a–c in the cases when the IR capability is activated, when the active power starts to decrease at the moment the frequency fault occurs, the shape of the signal eventually forms 'a peak', reaching values of approximately 0.02 pu and 0.57 pu.

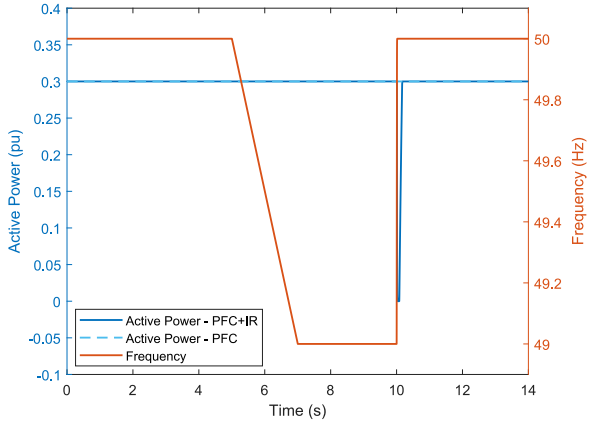

(a) Test case 4: $0.25P_N < P < 0.5P_N$

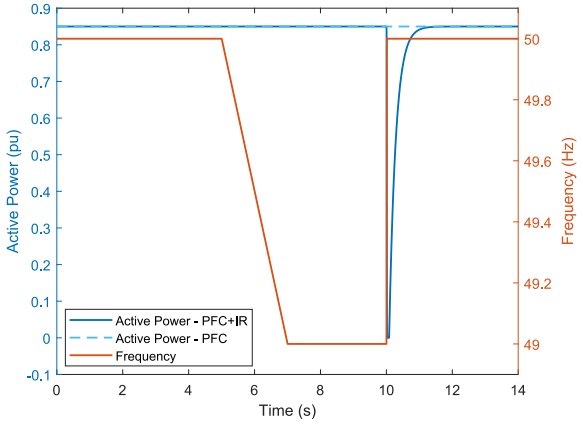

(b) Test case 5: $P > 0.80P_N$

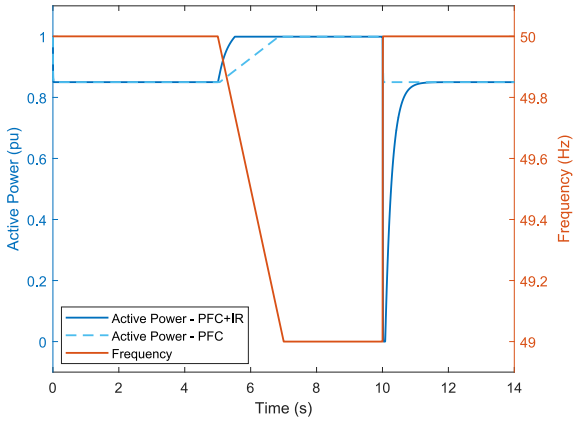

(c) Test case 6: $P = 85\%P_N; P_{av} = P_N$

Fig. 6. Synthetic inertia capability of the PV system - PFC and combined PFC & IR to frequency decreases.

However, when the inertia module is deactivated, the power signal decreases, in accordance with the statism defined, at a constant rate until it reaches the new setpoint, showing no 'power peak'. It is therefore logical that the settling times obtained are lower for the tests in which the inertia module is not activated. These 'power peaks' appear as a consequence of the PV system's implemented response to frequency variations. Hence, once the frequency stops varying (reaches its maximum value), i.e. when the rate of change of frequency is zero, the IR 'added' to the PFC disappears and the PV system injects the amount of active power corresponding to this new frequency value. In test case 6 (Fig. 6c), there is no overshoot at the beginning of the frequency variation because the maximum power the PV system can deliver is 1 pu, and this limit is reached before the frequency has dropped to its minimum value.

The steady-state time is closely related to the settling time, since it starts once the settling time finishes and lasts as long as the system operates in its new steady-state condition. Therefore, under frequency increases (Table 3 and Fig. 5), it is observed, both numerically and graphically, that the steady-state time is higher when the inertia module is disabled. This makes sense, given that, in both cases, the new steady-state operating point ends at the same time but the settling times are lower with the inertia module disabled. The exact opposite occurs, however, in test case 6, under a frequency decrease, since in this case the signal remains longer in its new steady-state condition when the inertia module is activated (see Fig. 6c and Table 4).

Finally, the measured ramp-down times are very low in all cases (in the order of the hundredth, see Tables 3 and 4), and are, in all test cases in which there was a change in the output power and, hence, a subsequent recovery (this only happens in test case 6, see Fig. 6c), lower when the inertia module is activated. Summarizing, it can be stated that the implementation of the inertia module substantially reduces the PV system's response times to changes in frequency.

In particular, under frequency increases, the reaction time is reduced by at least 84% in all test cases, while the response time is reduced by more than 68% in the worst case and by more than 80% in the best case. Under frequency decreases, the reaction time is reduced by 83%, and the response time is reduced by 73%. Taking into account that the current criteria for considering that solar PV systems comply with the synthetic inertia requirement is that the reaction and response times are lower when the inertia module is activated, it can be stated that in the case analyzed herein, the PV power converter that forms part of the system complies with this requirement.

4.2. *Evaluation of the inertial response at power plant level*

Tables 5 and 6 show the numerical results obtained once the required tests and measurements have been conducted, this time at the power plant level. As indicated previously, a power plant controller also forms part of the PV facility, and thus has an influence on the results. Table 5 shows the results under frequency increases test cases, and Table 6 shows the results under frequency decreases test cases. As in the previous test cases, in these tables, the comparison of the variables in italics,

Table 5
Numerical results of the inertia emulation test cases under frequency increases. Evaluation at the PCC.

Frequency Increases						
Test Case	7		8		9	
P Range (Test Case)	$0.25P_N < P < 0.50P_N$		$P > 0.80P_N$		$P = 90\%P_N$ $P_{av} = P_N$	
Inertia Emulation	No	Yes	No	Yes	No	Yes
Default *P* Boost, Δ*P* (pu)	−0.16	−0.16	−0.16	−0.16	−0.16	−0.16
Gradient of *P* Boost, *dP*/*dt* (pu/s)	−0.06	−0.04	−0.06	−0.04	−0.06	−0.04
Reaction Time (s)	1.33	0.05	1.33	0.05	1.33	0.05
Response Time (s)	3.53	3.78	3.55	3.77	3.55	3.80
Settling Time (s)	3.53	3.78	3.55	3.77	3.55	3.80
Steady-State Time (s)	3.47	3.22	3.45	3.20	3.45	3.20
Ramp-down Time (s)	2.00	0.01	2.01	0.01	2.02	0.00
Recovery Time (s)	0.00	2.20	0.00	2.22	0.00	2.28

Table 6
Numerical results of the inertia emulation test cases under frequency decreases. Evaluation at the PCC.

Frequency Decreases						
Test Case	10		11		12	
P Range (Test Case)	$0.25P_N < P < 0.50P_N$		$P > 0.80P_N$		$P = 90\%P_N$ $P_{av} = P_N$	
Inertia Emulation	No	Yes	No	Yes	No	Yes
Default *P* Boost, Δ*P* (pu)	0.00	0.00	0.00	0.00	0.10	0.10
Gradient of *P* Boost, *dP*/*dt* (pu/s)	0.00	0.00	0.00	0.00	0.05	0.03
Reaction Time (s)	0.00	0.00	00.00	0.00	1.39	0.04
Response Time (s)	0.00	0.00	0.00	0.00	3.31	3.37
Settling Time (s)	0.00	0.00	0.00	0.00	3.31	3.37
Steady-State Time (s)	0.00	0.00	0.00	0.00	3.70	3.27
Ramp-down Time (s)	0.00	0.00	0.00	0.00	2.07	0.00
Recovery Time (s)	0.00	0.05	0.00	0.19	0.00	2.30

both with the inertia module enabled and disabled, determines the compliance of the evaluated system with the synthetic inertia requirement.

Graphically, the simulation responses of the PV power plant are shown in Fig. 7 under frequency increases and Fig. 8 under frequency decreases. As in Figs. 5 and 6, orange represents frequency, dark blue represents the active power response of the PV power plant when both the PFC and the IR capabilities are considered in the control algorithms that manage the PV system, and blue dotted lines represent the active power response of the PV power plant when the PV system only contributes to PFC in the network. The tolerance band is also shown, as an example in the test cases at power plant level, in Fig. 7a, in light gray.

Tables 5 and 6 show that the reaction time when the inertia emulation is enabled is lower, both under frequency increases and decreases, than the reaction time when the inertia emulation module is disabled. This is also in line with the values of the gradient of *P* boost, which are lower in the cases in which an IR is provided by the PV system. Thus, for the same default *P* boost value, it can be stated that the power plant starts contributing more quickly to the PFC in the network when the PV system's synthetic inertia module is activated. This can be observed graphically in Figs. 7a–c and 8c. However, it can also be observed that, although power starts to decrease (in the cases under frequency increases), then it suddenly rises again, only to fall again and suffer another setback. This pattern of behavior is repeated in all the tests in which there is a change in the power plant's power response during the frequency disturbance (Figs. 7a–c and 8c), and causes the response time to be longer when the inertia module is activated (Tables 5 and 6). The settling time of the PV power plant response under frequency variations is also longer when the inertia emulation module is enabled, and this happens for the same reason as explained above.

The 'rises and falls' in power at the beginning of the frequency fault, which can be perfectly observed in Fig. 7a–c and 8c when an IR response is provided by the PV systems and the PPC -remember that the PPC also has the capacity to give an inertial response, as indicated in Section 3.3, are due to the communication time of the control devices. In other words, when the frequency disturbance occurs, it is detected by both the PV power conversion systems and the PPC. The PV systems then automatically start to act according to their control algorithms, increasing or decreasing the power they inject accordingly. However, the PPC has not yet sent the control signal to the PV systems to act –it has not yet had time, so the PPC is somehow 'telling' the PV systems not to modify their output power yet. Using test case 7 as an example (Fig. 7a), this is why a returning of the power signal is observed after the first drop. At the same time, the PV systems' control algorithms are still detecting the frequency variation and therefore continue to send orders for action, hence the following power drop. This is repeated several times until the control signal sent by the PPC reaches the PV systems, and power decreases 'cleanly'.

Regarding the steady-state time, it is, in all cases, lower when the synthetic inertia module is enabled. This is because, as it takes the power plant longer to reach its new operating point when providing an IR, the time it spends operating at that new setpoint is shorter. This can also be clearly observed in Fig. 7a–c and 8c.

The values of the ramp-down and recovery times are correlated. As can be observed in Fig. 7a–c and 8c, when inertia is not emulated (blue dotted lines), power gradually recovers, after the fault, until the pre-fault active power value is reached again. Thus, no recovery periods are observed in these cases, and the ramp-down values obtained are around 2 s. In contrast, when inertia is emulated (blue solid lines), power recovers very quickly, which is why ramp-down time values are around 0 s. However, it then presents a marked recovery period, since power again deviates from the pre-fault setpoint. In these cases, recovery periods are around two and half seconds. Recovery periods appear in the cases where inertia is emulated because, as in the case where the response is analyzed exclusively at the at the power conversion PV system level (Section 4.1), the PV system and the PPC detect both frequency increases and decreases and, hence, provides an IR at the beginning and the end of the frequency disturbance. Thus, power varies proportionally to the time derivative of frequency in both cases.

Regarding test cases 10 and 11 (Table 6), the reaction, response, settling, steady-state and ramp-down times are 0 when the synthetic inertia module is both enabled and disabled. As observed in Fig. 8a and b, all these time values are 0 because there is no change in the active power output of the PV power plant when the frequency disturbance occurs. This is because, as in the case of some of the test cases conducted at the power conversion PV system level (Section 4.1), the PV system has no more power to deliver than the power at which the analyses are conducted, i.e., there is no more primary resource available and therefore the PV power converter cannot inject more power than it already does.

It can be stated that the implementation of the inertia module in the PPC is of no benefit. As observed in Tables 5 and 6, although reaction times are lower because power starts to vary immediately when the frequency fault occurs, because then the power sets back several times due to the contradictory control signals received by the PV power converters, the response times are eventually longer when the synthetic inertia emulation module is enabled. Therefore, in order to provide IR at power plant level and allow for faster power-frequency regulation in the network, the PPC should not act, since in this case it disturbs the PV power converter's behavior. In general, dynamic power plant responses should not go through the PPC because they slow down the actuation processes.

5. Conclusions

As the integration of renewable power installation grows, power

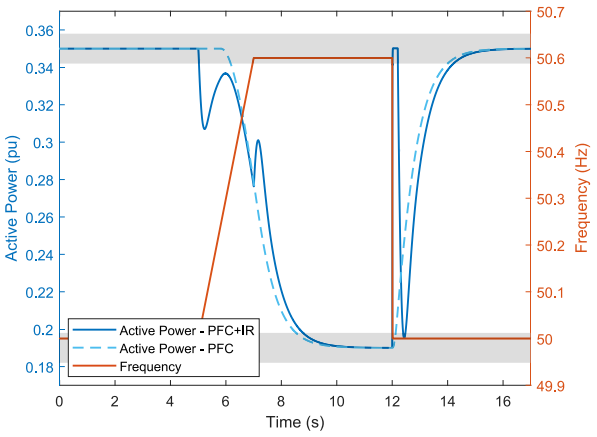

(a) Test case 7: $0.25P_N < P < 0.5P_N$

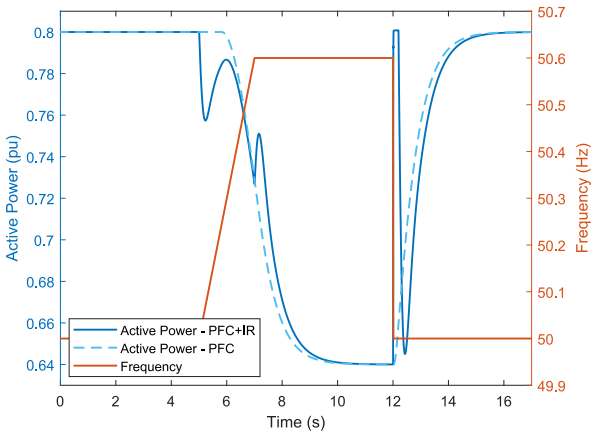

(b) Test case 8: $P > 0.80P_N$

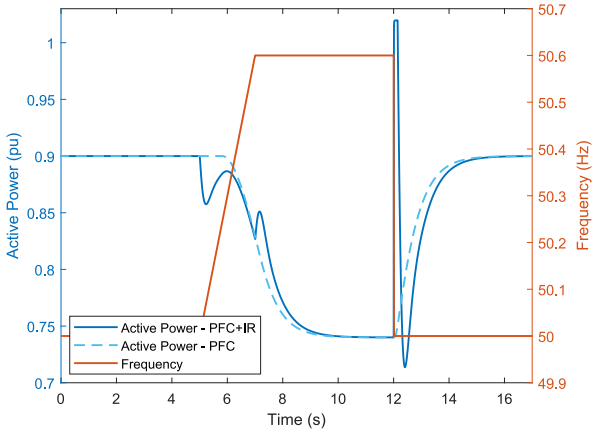

(c) Test case 9: $P = 90\%P_N; P_{av} = P_N$

Fig. 7. Synthetic inertia capability of the power plant - PFC and combined PFC & IR to frequency increases.

systems' inertia is reduced, and this makes frequency changes faster. This forces systems to also have to provide a faster response to mitigate the effects of frequency disturbances, which is a great challenge that has to be addressed jointly by the different entities involved in the processes of generation, transmission and distribution of electricity. Spain is currently the only country that has already included, in its grid code, the possibility for PV power plants and other renewable installations to contribute to the regulation of power-frequency in the network in a similar way to conventional power plants: by providing an IR. Moreover, Spain has also defined the methodology to be followed to check whether a PV power plant complies with this 'synthetic inertia' requirement. Compliance with this requirement is still optional, although all the indications are that it will be mandatory in the near future.

Under this framework, the present contribution analyzes the responses of an actual PV power plant located in Spain when the synthetic inertia requirement is evaluated according to the Spanish grid code. The IR of the power plant is assessed when measurements are conducted at the at the power conversion PV system level -which is the device equipped with the control algorithms that allow an IR to be provided, and at the power plant level, i.e., at the PCC. In this latter case, in addition to the PV power converter, the overall facility response is also influenced by a PPC.

When carrying out the different analyses established in the Spanish normative document, a series of variables must be measured. Among these, the response time of the PV system power signal –and of the power plant, as appropriate– is measured. This is done when the inertia emulation module implemented in the PV system is enabled and disabled. In this way, the speed of the power-frequency regulation in the network in both situations is evaluated. If the response times obtained when the module is activated are shorter, the synthetic inertia requirement is considered to be met.

At the at the power conversion PV system level, the implementation of the inertia emulation module substantially reduces the response time values obtained. It can thus be affirmed that the PV system under consideration complies with the synthetic inertia technical requirement established in the Spanish grid code. In contrast, at the plant level, the actuation of the PPC interferes with the response of the PV system, distorting it and causing the response times to be longer with the inertia module activated. Thus, a clear conclusion from this study is that the PPC should not influence the dynamic responses of the power plant, as this produces the opposite effect to that desired, contributing more quickly to power-frequency regulation.

This article, which provides a realistic vision in its field of study, also highlights the importance of the use of dynamic simulation models for the analysis of the compliance of renewable installations with the different requirements established in grid codes. It also highlights the importance of developing a specific document to carry out the compliance analysis tests of solar PV facilities with the synthetic inertia technical requirement, since, thus far, they have been based on what has been developed for wind power plants.

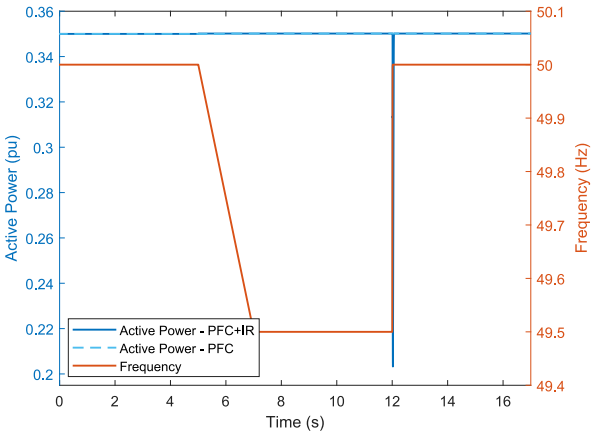

(a) Test case 10: $0.25P_N < P < 0.5P_N$

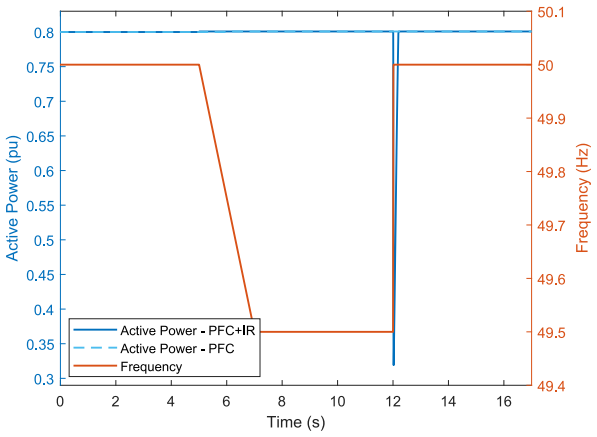

(b) Test case 11: $P > 0.80P_N$

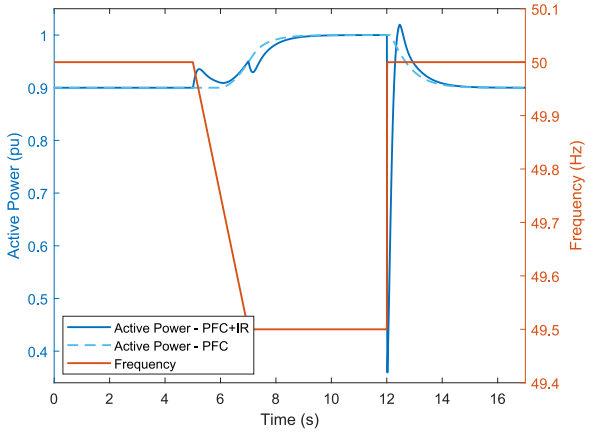

(c) Test case 12: $P = 90\%P_N; P_{av} = P_N$

Fig. 8. Synthetic inertia capability of the power plant - PFC and combined PFC & IR to frequency decreases.

CRediT authorship contribution statement

Raquel Villena-Ruiz: Methodology, Software, Validation, Writing – original draft, Writing – review & editing. **Andrés Honrubia-Escribano:** Conceptualization, Methodology, Supervision, Writing – review & editing. **Jesús C. Hernández:** Conceptualization, Methodology, Supervision, Writing – review & editing. **Emilio Gómez-Lázaro:** Conceptualization, Methodology, Supervision, Writing – review & editing.

Declaration of Competing Interest

The authors declare that they have no known competing financial interests or personal relationships that could have appeared to influence the work reported in this paper.

Data availability

The data that has been used is confidential.

Acknowledgements

This research was partially funded by the Council of Communities of Castilla La Mancha (Junta de Comunidades de Castilla-La Mancha, JCCM) through project SBPLY/19/180501/000287; by the Council of Andalucía (Junta de Andalucía. Consejería de Transformación Económica, Industria, Conocimiento y Universidades. Secretaría General de Universidades, Investigación y Tecnología) through project ProyExcel_00381. The work was also partially supported by the Spanish Ministry of Science and Innovation, the European Union and the State Research Agency (Agencia Estatal de Investigación, AEI) through projects PID2021-126082OB-C21 and PID2021-126082OB-C22. The authors also acknowledge the support provided by the Thematic Network 723RT0150 "Red para la integración a gran escala de energías renovables en sistemas eléctricos (RIBIERSE-CYTED)" financed by the call for Thematic Networks of the CYTED (Ibero-American Program of Science and Technology for Development) for 2022.

References

[1] IEA. Introduction to system integration of renewables, Tech. rep., International Energy Agency (IEA); 2020.
[2] European Commission. COMMISSION REGULATION (EU) 2016/631 of 14 April 2016 establishing a network code on requirements for grid connection of generators, Tech. rep., European Commission; 2016.
[3] European Commission. COMMISSION REGULATION (EU) 2016/1388 of 17 August 2016 establishing a Network Code on Demand Connection., Tech. rep., European Commission; 2016.
[4] European Commission. COMMISSION REGULATION (EU) 2016/1447 of 26 August 2016 establishing a network code on requirements for grid connection of high voltage direct current systems and direct current-connected power park modules., Tech. rep., European Commission; 2016.
[5] Ministerio para la Transición Ecológica y el Reto Demográfico, Real Decreto 647/2020, de 7 de julio, por el que se regulan aspectos necesarios para la implementación de los códigos de red de conexión de determinadas instalaciones eléctricas. Tech. rep., Ministerio para la Transición Ecológica y el Reto Demográfico 2020.

[6] Ministerio para la Transición Ecológica y el Reto Demográfico, Orden TED/749/2020, de 16 de julio, por la que se establecen los requisitos técnicos para la conexión a la red necesarios para la implementacíon de los códigos de red de conexión. Tech. rep., Ministerio para la Transición Ecológica y el Reto Demográfico 2020.
[7] Red Eléctrica de Españ̃a. Norma técnica de supervisión de la conformidad de los módulos de generación de electricidad según el Reglamento UE 2016/631. Tech. rep., Red Eléctrica de Españ̃a 2021.
[8] Sarasua JI, Martínez-Lucas G, García-Pereira H, Navarro-Soriano G, Molina-García Á, Fernández-Guillamón A. Hybrid frequency control strategies based on hydro-power, wind, and energy storage systems: application to 100% renewable scenarios. IET Renew Power Gener 2022;16(6):1107–20.
[9] Sarojini RK, Palanisamy K, De Tuglie E. A fuzzy logic-based emulated inertia control to a supercapacitor system to improve inertia in a low inertia grid with renewables. Energies 2022;15(4):1333.
[10] International Energy Agency. Photovoltaic Power Systems Programme, Snapshot of Global PV Markets 2022, Tech. rep., International Energy Agency; 2022.
[11] International Energy Agency. Photovoltaic Power Systems Programme, Snapshot of Global PV Markets 2023, Tech. rep., International Energy Agency; 2023.
[12] Lopez A, Ogayar B, Hernández J, Sutil F. Survey and assessment of technical and economic features for the provision of frequency control services by household-prosumers. Energy Policy 2020;146:111739.
[13] Tamrakar U, Shrestha D, Maharjan M, Bhattarai BP, Hansen TM, Tonkoski R. Virtual inertia: current trends and future directions. Appl Sci 2017;7(7):654.
[14] Fernández-Guillamón A, Gómez-Lázaro E, Muljadi E, Molina-García Á. Power systems with high renewable energy sources: a review of inertia and frequency control strategies over time. Renew Sustain Energy Rev 2019;115.
[15] Yap KY, Sarimuthu CR, Lim J-M-Y. Virtual inertia-based inverters for mitigating frequency instability in grid-connected renewable energy system: a review. Appl Sci 2019;9(24):5300.
[16] Kushwaha P, Prakash V, Bhakar R, Yaragatti UR. Synthetic inertia and frequency support assessment from renewable plants in low carbon grids. Electr Pow Syst Res 2022;209:107977.
[17] Prakash V, Kushwaha P, Sharma KC, Bhakar R. Frequency response support assessment from uncertain wind generation. Int J Electr Power Energy Syst 2022;134:107465.
[18] Nema S, Prakash V, Pandžić H. Adaptive synthetic inertia control framework for distributed energy resources in low-inertia microgrid. IEEE Access 2022;10:54969–79.
[19] Khazaei J, Tu Z, Liu W. Small-signal modeling and analysis of virtual inertia-based pv systems. IEEE Trans Energy Convers 2020;35(2):1129–38.
[20] Peng Q, Yang Y, Liu T, Blaabjerg F. Coordination of virtual inertia control and frequency damping in pv systems for optimal frequency support. CPSS Trans Power Electron Appl 2020;5(4):305–16.
[21] Sarojini RK, Kaliannan P, Teekaraman Y, Nikolovski S, Baghaee HR. An enhanced emulated inertia control for grid-connected pv systems with hess in a weak grid. Energies 2021;14(6):1721.
[22] Karpana S, Batzelis E, Maiti S, Chakraborty C. Pv-supercapacitor cascaded topology for primary frequency responses and dynamic inertia emulation. Energies 2021;14(24):8347.
[23] Yang L, Hu Z, Xie S, Kong S, Lin W. Adjustable virtual inertia control of supercapacitors in pv-based ac microgrid cluster. Electr Pow Syst Res 2019;173:71–85.
[24] Ramos JG, Araújo RE, Virtual inertia and droop control using dc link in a two-stage pv inverter. In: 2020 IEEE 14th International Conference on Compatibility, Power Electronics and Power Engineering (CPE- POWERENG), vol. 1, IEEE; 2020. p. 55–60.
[25] Su Y, Li H, Cui Y, You S, Ma Y, Wang J, et al. An adaptive pv frequency control strategy based on real-time inertia estimation. IEEE Trans Smart Grid 2020;12(3):2355–64.
[26] Peng Q, Tang Z, Yang Y, Liu T, Blaabjerg F. Event-triggering virtual inertia control of pv systems with power reserve. IEEE Trans Ind Appl 2021;57(4):4059–70.
[27] Bueno PG, Hernández JC, Ruiz-Rodriguez FJ. Stability assessment for transmission systems with large utility-scale photovoltaic units. IET Renew Power Gener 2016;10(5):584–97.
[28] Hernández JC, Bueno PG, Sánchez-Sutil F. Enhanced utility-scale photovoltaic units with frequency support functions and dynamic grid support for transmission systems. IET Renew Power Gener 2017;11(3):361–72.
[29] Martínez-Lavín M, Villena-Ruiz R, Honrubia-Escribano A, Hernández JC, Gómez-Lázaro E. Evaluation of the latest spanish grid code requirements from a pv power plant perspective. Energy Rep 2022;8:8589–604.
[30] Martínez-Lavín M, Villena-Ruiz R, Honrubia-Escribano A, Hernández JC, Gómez-Lázaro E. Proposal for an aggregated solar pv power plant simulation model for grid code compliance. Electr Pow Syst Res 2022;213.
[31] Ledesma Larrea P. Ańalisis dińamico y control de sistemas eléctricos; 2020.
[32] ENTSO-E. 2021 Load-Frequency Control Annual Report, Tech. rep., European Network of Transmission System Operators for Electricity (ENTSOE); 2022.
[33] NREL. Inertia and the Power Grid: A Guide Without the Spin, Tech. rep., National Renewable Energy Laboratory (NREL); 2022.
[34] Zhang W, Cantarellas AM, Rocabert J, Luna A, Rodriguez P. Synchronous power controller with flexible droop characteristics for renewable power generation systems. IEEE Trans Sustainable Energy 2016;7(4):1572–82.
[35] Kimbark E. Power system stability. John Wiley and Sons; 1948.
[36] Vittal V, McCalley JD, Anderson PM, Fouad A. Power system control and stability. John Wiley & Sons; 2019.
[37] IEC 61400-21-1. Wind energy generation systems - Part 21-1: measurement and assessment of electrical characteristics - Wind turbines; 2019.
[38] Villena-Ruiz R, Honrubia-Escribano A, Jiménez-Buendía F, Sosa Avendaño J, Frahm S, Gartmann P, Fortmann J, Sørensen P, Gómez-Lázaro E. Extensive model validation for generic IEC 61400-27-1 wind turbine models. Int J Electr Power Energy Syst 2022;134:107331.
[39] Nanou SI, Papakonstantinou AG, Papathanassiou SA. A generic model of two-stage grid-connected pv systems with primary frequency response and inertia emulation. Electr Pow Syst Res 2015;127:186–96.
[40] Cabrera-Tobar A, Bullich-Massagué E, Aragüés-Peñalba M, Gomis-Bellmunt O. Topologies for large scale photovoltaic power plants. Renew Sustain Energy Rev 2016;59:309–19.
[41] Xiao W. Photovoltaic power system: modeling, design, and control. John Wiley & Sons; 2017.
[42] Hassaine L, OLias E, Quintero J, Salas V. Overview of power inverter topologies and control structures for grid connected photovoltaic systems. Renew Sustain Energy Rev 2014;30:796–807.
[43] ENTSO-E. Network code on requirements for grid connection applicable to all generators, Tech. rep., European Network of Transmission System Operators for Electricity (ENTSO-E); 2015.